

SELF PROPAGATING HIGH TEMPERATURE (SHS) FOR SYNTHESIS OF COMPLEX HARD FERRITE

M.B.Morsi

CMRDI, P.O.BOX 87, Helwan ,Cairo,Egypt

ABSTRACT

A mixture of barium oxide (BaO_2), iron (III) oxide Fe_2O_3 , chromium (III) oxide (Cr_2O_3) and iron powder is subjected to thermal initiation in air (oxygen atmosphere). This produces a self propagating reaction (SHS) with velocity of 1 mm s^{-1} and the formation of predominantly $\text{BaFe}_{12-x}\text{Cr}_x\text{O}_{19}$. SHS followed by annealing at 1200°C for 2h gives a crystalline phase powder of ferrite material. The products were characterized by XRD analysis, FTIR spectra and SEM. The hysteresis loops of the products were also recorded to determine the magnetic properties of the synthesised ferrite.

Keywords: Self propagation synthesis (SHS), ferrite synthesis, characterization and magnetic properties.

INTRODUCTION

Ferrite materials are made by one of the two major routes, either by a dry traditional ceramic heat and heat approach[1,2] or by a wet co-precipitation[1, 3] or sol-gel type process[4]. These conventional techniques invariably involve multiple grinding, heating and cooling process[5]. Reaction usually requires extensive time periods because interdiffusion of reacting solids is slow even at high temperature[6].

A relatively new synthetic variant has been developed which negates the need to externally heat a reaction. This is based on self-propagating reactions which provide the energy to overcome the solid-state diffusion barrier internally, within the starting materials, by promoting an exothermic chemical reaction. This process is termed self-propagating high temperature synthesis SHS[7]. Recently, it has been shown that SHS is an ideal technique for synthesis of many types of ferrites[8, 9].

The aim of this paper is to utilize SHS technique for formation of complex hard ferrite $\text{BaFe}_{12-x}\text{Cr}_x\text{O}_{19}$.

EXPERIMENTAL

The reagents used were obtained from BDH chemical company. Weighing grinding and mixing for the starting materials were performed under a nitrogen atmosphere in a Safforn Scientific glove box. SHS reactions were carried out in air under a flow of oxygen gas on a ceramic tile. The reactions were initiated by a heated filament (800°C) and wave propagation was determined by using imaging Camera of type FLIR. Photographs of the solid flame produced on initiating mixture of starting materials are shown in Figure 1. Sintering was carried out in a Carbolite rapid heating furnace with heating and cooling rates of 20°C min⁻¹. Samples were ground after the SHS reaction and also after sintering, and all the measurements were recorded on powder samples. The sintered products were investigated by FT – IR spectra, XRD analysis and Scanning electron microscopy (SEM). XRD analysis was performed on a Philips X-Pert Diffraction using Cu K α radiation ($\lambda_1 = 1.5405 \text{ \AA}$, $\lambda_2 = 1.5443 \text{ \AA}$). FT – IR spectra were obtained by using a Perkin – Elmer 1710 instrument of DTGS detector and DRIFT accessory with micro – sampler. The products were investigated in KBr powder as reference material. Micrographs of the obtained products were performed by SEM of type Hitachi S – 4000.

Vibrating sample magnetometry was carried out on a Aerosonic 3001

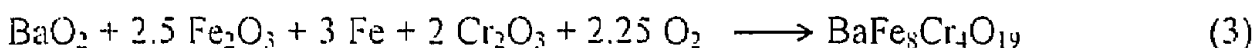
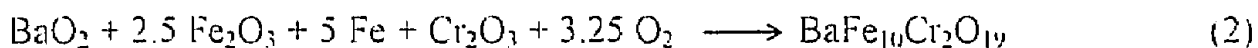
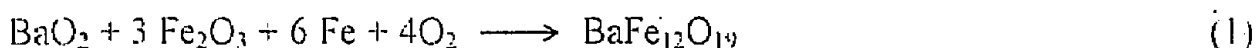
magnetometer at room temperature in applied field up to 7.5 Koe.

Preparation of $\text{BaFe}_{12-x}\text{Cr}_x\text{O}_{19}$ $x = (0,2,4)$

Barium peroxide (BaO_2), iron powder, iron oxide Fe_2O_3 and chromium oxide (Cr_2O_3) were ground together in a pestle and mortar. The resulting powder was placed on a ceramic tile in air and the mixture was initiated at one end by filament at about 800°C . This produced an orange wave (SHS reaction) passing through the material with speed 1 mm s^{-1} . The powder darkened to black after the propagation wave had passed and become partly fused. The black material after sintering at 1200°C for 2h was analysed by XRD and FT – IR spectra. The morphology of the formed ferrites were investigated by SEM.

RESULTS AND DISCUSSIONS

SHS reactions were performed by using various starting mixtures of Fe_2O_3 , BaO_2 , Fe and Cr_2O_3 . The molar ratio of each reagent was chosen to conform with the stoichiometry in the products (Table 1) according to the equations:



In these SHS reactions a slight excess of BaO_2 was used which act as a

source of oxygen. The reaction was driven by the exothermic oxidation of Fe metal and the other oxides act as heat sink to stop the reaction becoming too exothermic, with incorporation in the product. The peroxide was used in preference to the carbonate, which is used in conventional synthesis of ferrite. The peroxide provides a good source of oxygen and also avoid potential carbon contamination[9].

It is noticed that the SHS reactions are rapid and over in a few seconds and in all reactions the product was a black – brown material. Traditional methods to use materials involve the use of ball mills to grind the reagents[10] or precipitation synthesis in which many individual reactions steps are needed to finish this process[11].

Characterization

XRD analysis was performed for all the unsintered and sintered SHS products. The unsintered products showed predominantly $\text{BaFe}_{12-x}\text{Cr}_x\text{O}_{19}$ with small amounts of metal oxide impurities such as Fe_2O_3 and Cr_2O_3 , (Figure 2a). The presence of these phases shows incomplete reaction during the SHS stages. Sintering process largely removed these impurities (Figure 2b). By applying Sherrer equation[12] and from the line broadening of many peaks, neglecting strain effects. The corrections of 2θ and the intensities of full width half maximum

(IFWHM) were calculated. The resulting average crystallite size was 47 nm. This value is smaller than obtained by parkin et al[9]. In some of Cr- rich SHS samples, a trace amounts of Fe_2O_3 and Cr_2O_3 impurities were noted even after sintering. Also XRD data showed hexagonal structure for $\text{BaFe}_{12-x}\text{Cr}_x\text{O}_{19}$ with a decrease in lattice parameters with increasing Cr – substituted as shown from Table 2. The resulting variation in unit cell size may be attributed to the slightly smaller ionic radii of Cr^{3+} compared to that of Fe^{3+} . This result is in agreement with that obtained by other authors[9].

The FT – IR spectra of $\text{BaFe}_{12-x}\text{Cr}_x\text{O}_{19}$ samples showed a fundamental two broad bands ($470 - 520 \text{ cm}^{-1}$) and ($600 - 620 \text{ cm}^{-1}$), Figure 3. Some changes in the shoulders of the broad bands were noted with Cr substitution. It is noticed that these materials show strong overlapping absorption in the region $400 - 700 \text{ cm}^{-1}$, this is attributed to Fe – O and Cr –O stretches. It was mentioned that IR data for these compounds match most closely those materials in which there is a random distribution of the Cr, Fe atoms within the octahedral sublattice[13]. This is somewhat different to most traditionally prepared ferrites where the longer synthesis times allow for local ordering of the atoms on the octahedral sites.

SEM micrographs, Figure 4 of the sintered $\text{BaFe}_{12-x}\text{Cr}_x\text{O}_{19}$ samples showed average crystallite size of 60 nm which is larger than obtained from XRD results.

As the dimensions are larger than that obtained from the X-ray data, this means that there may be some structural defects present in the grains.

Magnetic Properties

Hysteresis loops were recorded on the produced samples in field up to 7.5 Koe at room temperature. Representative hysteresis loops is shown in Figure 5. The variation in maximum magnetization σ_{max} , remanent magnetization σ_r and coercive force H_c with chromium substitution for $BaFe_{12-x}Cr_xO_{19}$ samples are shown in Figure 6. It is noticed that a steady decrease in the magnetization (σ_{max} and σ_r) as a function of Cr substitution increases up to $x = 4$. This indicates that a paramagnetic behaviour is obtained with increasing Cr content in the ferrite material. This result may be due to the different crystallographic sites for iron atoms in octahedral and tetrahedral of opposite spins in $BaFe_{12}O_{19}$ [14]. From the coercive force measurement, it is observed that the samples all have high coercive forces, which proves the significant property of hard ferrites $BaFe_{12-x}Cr_xO_{19}$.

CONCLUSIONS

Representative hard ferrites $BaFe_{12-x}Cr_xO_{19}$ were synthesized by self-propagating high-temperature synthesis (SHS) in air. The reactions are easy to perform and offer significant reductions in synthesis time and energy compared to conventional synthesis. Single phase products were obtained having average

crystallite size of 47 nm and SEM measurements showed larger crystallite size of 60 nm indicating that some structural defects are present in the grains.

Magnetic measurements for the produced samples by SHS technique indicated that these samples have high coercive forces which proves the significant of hard ferrites $\text{BaFe}_{12-x}\text{Cr}_x\text{O}_{19}$.

ACKNOWLEDGEMENT

The author thanks both the Hungarian Academy of Science and Research Laboratory of Material Science and Environmental Chemistry for this fellowship. Prof. Dr. J. Szépvölgy is thanked for help in XRD, SEM and Magnetic measurements and useful discussion. Thanks for Dr. B. Zelei for FT – IR spectra measurements. Thanks for Dr. Z. Károly for using imaging Camera FLIR and preparing SHS photographs.

REFERENCES

1. J. Smit and H P. J. Wijn, Ferrites, 1959, Wiley, New York.
2. D.A. Rawlinson, Ph.D Thesis, 1998, Brunel University,.
3. A. Goldman and A.M Laing, J. phys. 1976, vol. 4, no. 1, pp. 18-22.

4. J. Lirage, M. Henry and C. Sanchez, *J. Magn. Mater.*, 1993, vol. 18, pp. 214–220.
5. C.N. R. Rao and J. Gopalakrishanan, *New directions in solid state chemistry*, Cambirdge University press, Cambridge, 1997, pp. 122 - 129.
6. H. Yanagida, K. koumato and M. Migayuma, *The Chemistry of Ceram.*, J.Wiley and Sons, chichester, 1996. pp. 971 – 979.
7. A.G. Merzhanov, *Adv. Mater., Int. J.* 1992, vol. 4, pp. 294 - 301.
8. M.V. Kuznestesov, Q. A Pankhurst and I. P. Parkin *J. mater. Chem*; 1998, vol. 8, pp. 2701 – 2706.
9. M.V. Kuzenetsov, and I.P. Parkin and Q. A. Pankhurst, *J. Mater., Chem . .*, 1999, vol. 9, pp. 273 -281.
10. G. Elwin. I. P. Parkin, and Y.G. Morazov, *J. Mater Chem.*, 1998. vol. 8, pp. 573 - 578.
11. H. Yang, Z. Wang; M. Zhao, J. Wang. D Han, H. Luo and L. Wang, *J. Mater. Chem. Phys.*, 1997. vol. 48, pp. 60 - 66.

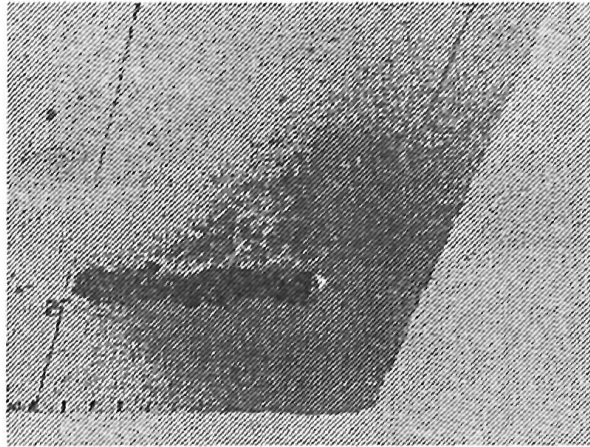
12. B.Z. Shakhashiri, *Chemical Demonstrations, a Handbook for Teachers of chemistry*, university of wisconsin press, London, 1983, vol. 1, , pp. 85
13. N.K. Gill and P K.Ruri, *Indian J. Pure Appl. Phys.*, 1985, vol. 23, pp. 71-76.
14. H. Hibst, *Angew, Chem, Int. Ed. Eng.*, 1982, vol. 21, pp. 270 - 278.

Table 1. Molar ratios of the components used in SHS of $\text{BaFe}_{12-x}\text{Cr}_x\text{O}_{19}$

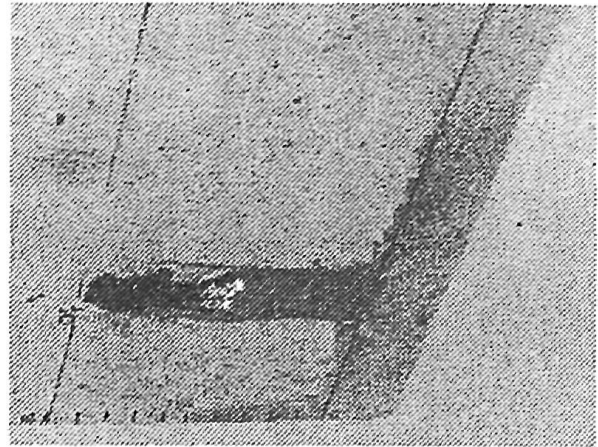
X	BaO_2	Fe_2O_3	Fe	Cr_2O_3
0	1.0	2.4	4.8	–
2	1.0	1.6	4.8	0.8
4	1.0	0.8	4.8	1.6

Table 2. XRD lattice parameter values of $\text{BaFe}_{12-x}\text{Cr}_x\text{O}_{19}$ prepared by SHS reactions.

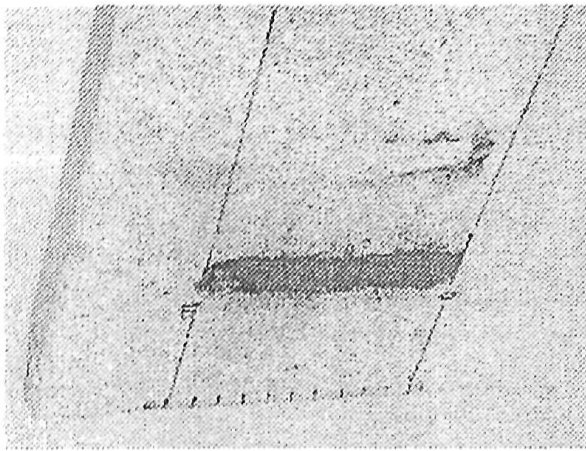
Ferrite	$a/\text{Å}^\circ$	$c/\text{Å}^\circ$
$\text{BaFe}_{12}\text{O}_{19}$	5.884	23.170
$\text{BaFe}_{10}\text{Cr}_2\text{O}_{19}$	5.871	23.082
$\text{BaFe}_8\text{Cr}_4\text{O}_{19}$	5.863	23.021



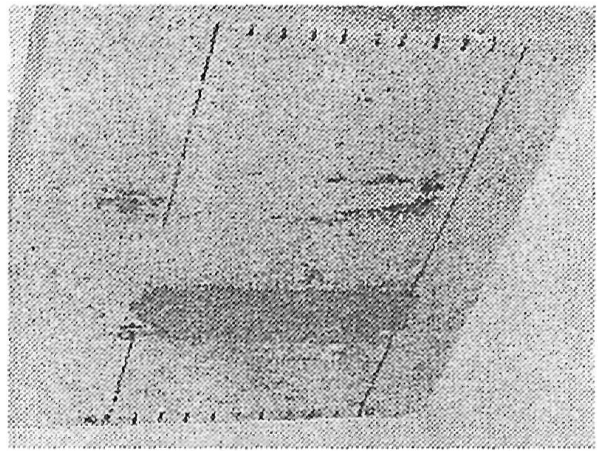
(a)



(b)



(c)



(d)

Fig. 1 Photographs of wave produced on initiating a mixture of BaO_2 , Fe_2O_3 , and Cr_2O_3 (1:1.6:4.8 molar ratio) at (a) time, = 0; (b) time = 50 second, (c) time = 90 second and (d) the end of SHS reaction. The mixture was initiated by a hot filament at the right side of powder.

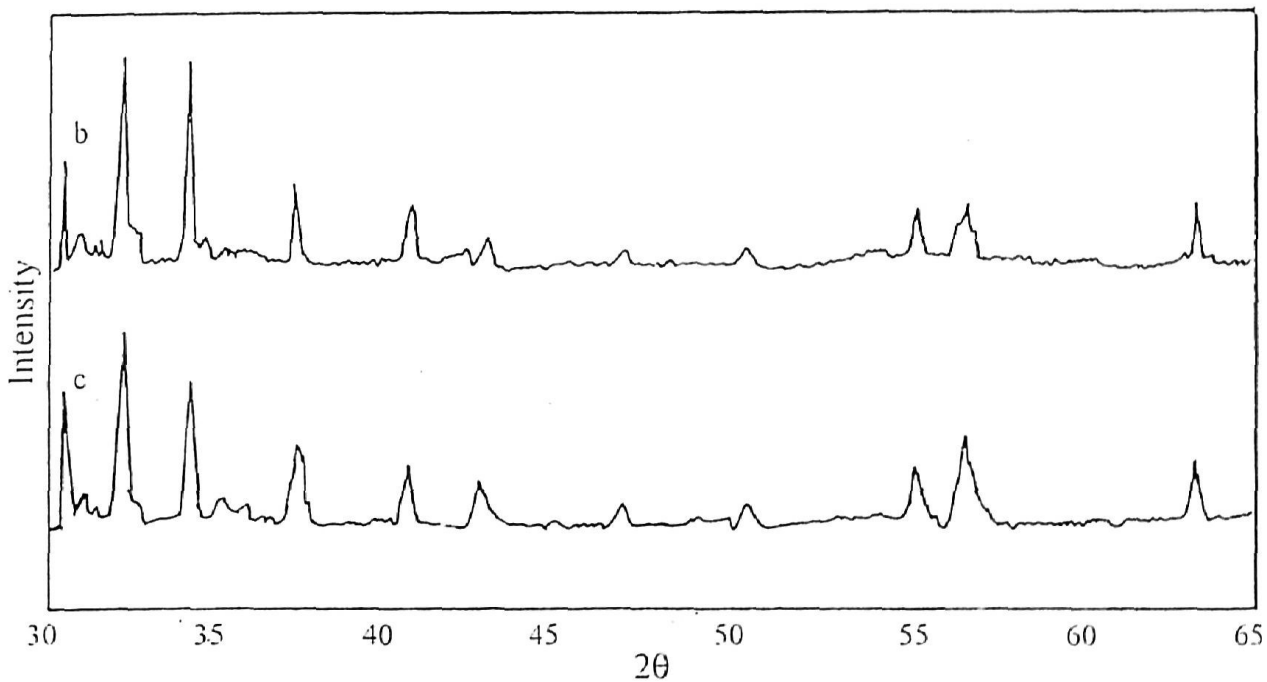
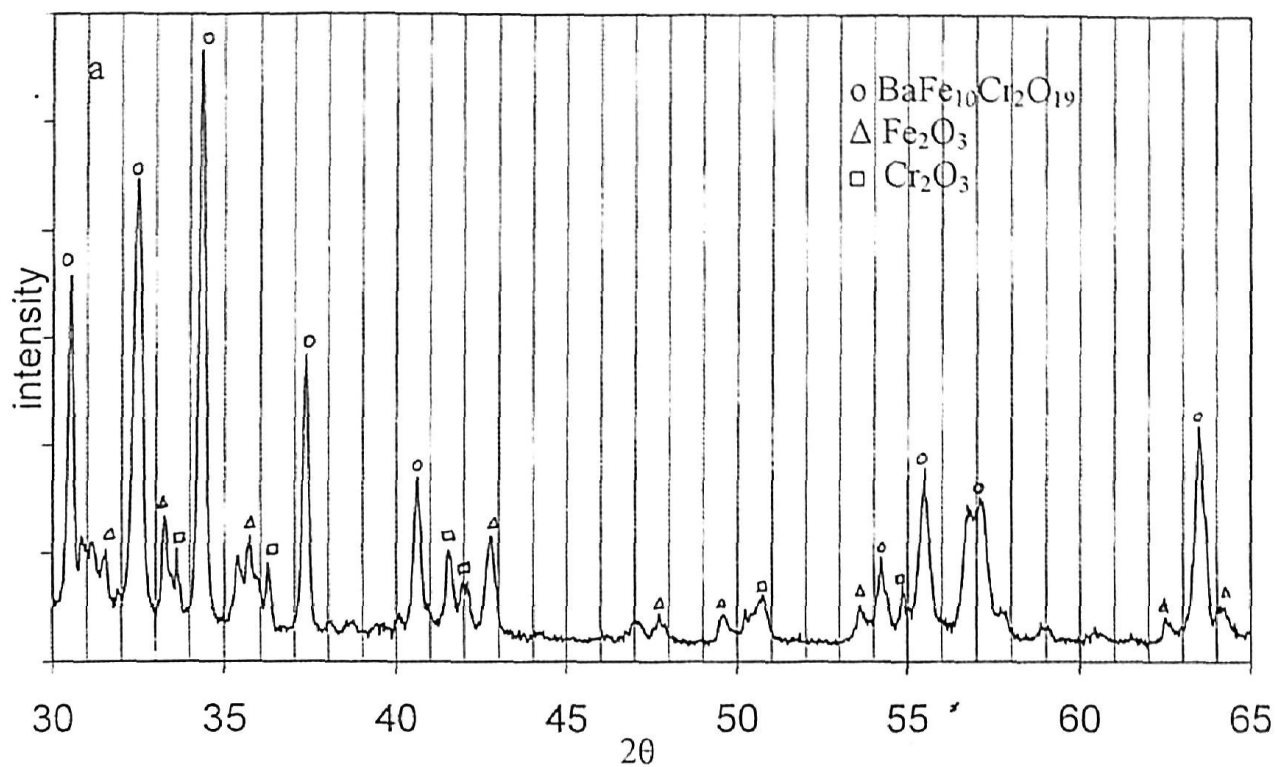


Fig. 2. X-ray diffraction pattern obtained from SHS reaction of BaO_2 , Fe_2O_3 , Fe and Cr_2O (1:1.6:4.8:0.8 molar ratio)

a- before sintering

b- after sintering 2h at 1200°C

c- XRD pattern of commercial sample $\text{BaFe}_{12}\text{O}_{19}$

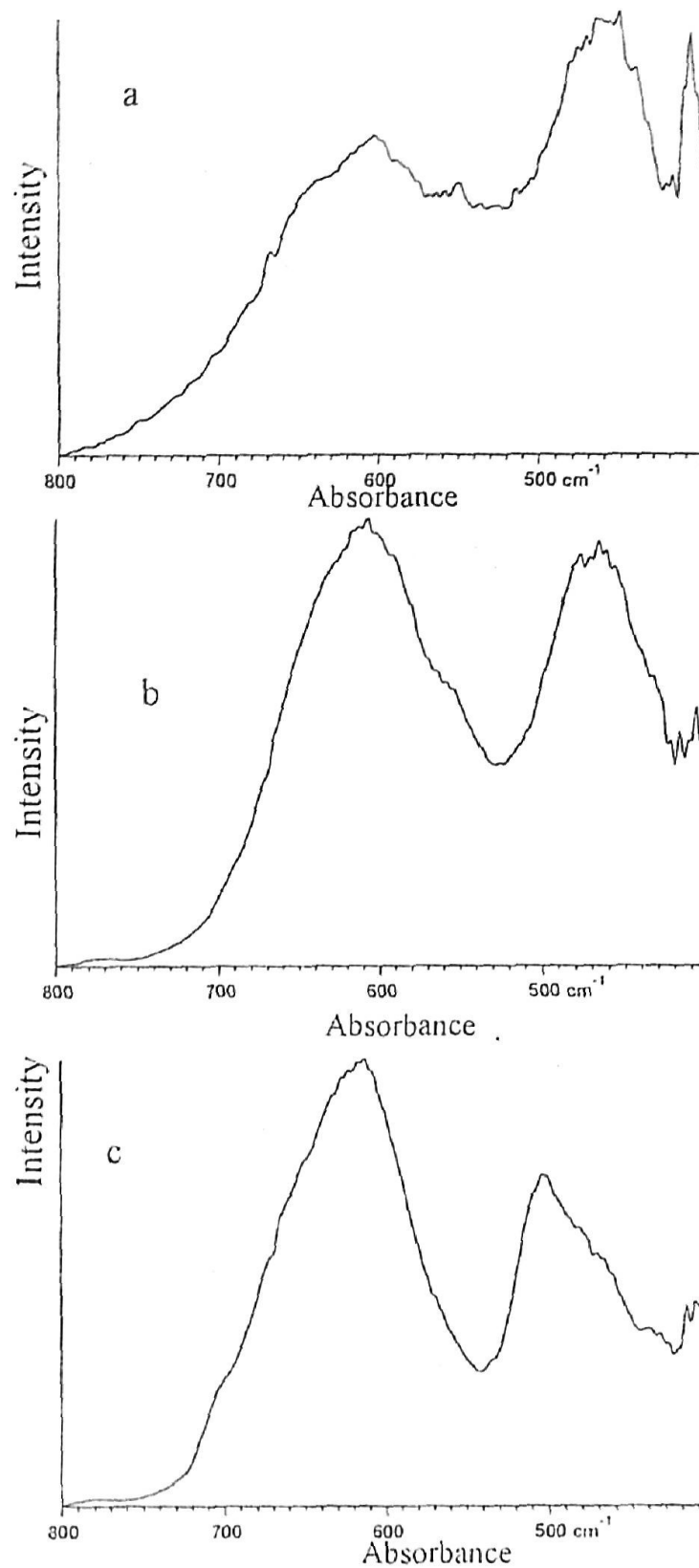


Fig. 3. FT – IR spectra of synthesized ferrites by SHS reactions,
 (a) $\text{BaFe}_{12}\text{O}_{19}$ (b) $\text{BaFe}_{10}\text{Cr}_2\text{O}_{19}$
 (c) $\text{BaFe}_8\text{Cr}_4\text{O}_{19}$

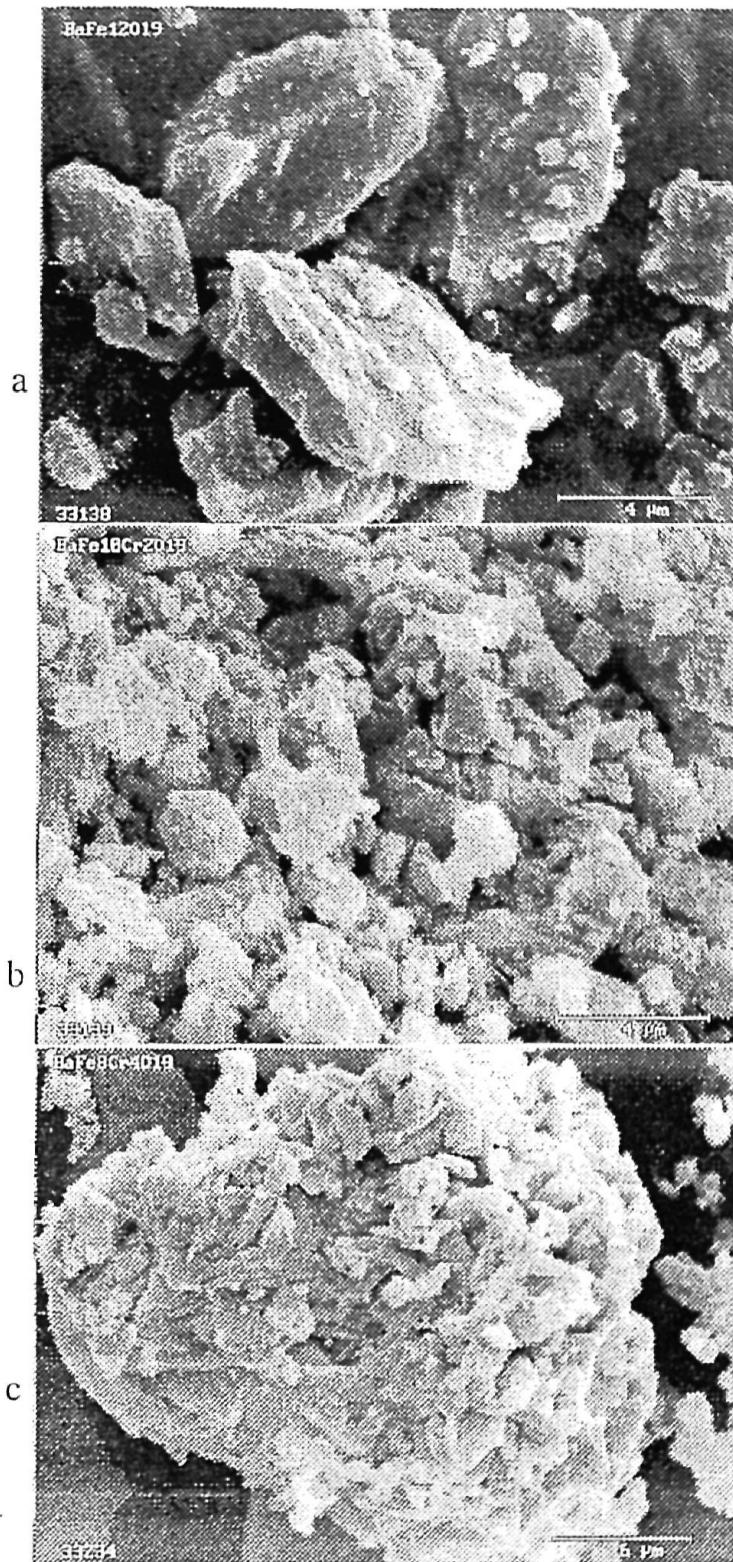


Fig. 4. SEM micrographs of synthesized ferrites by SHS reactions followed by sintering at 1200°C for 1 hr.

- (a) BaFe₁₂O₁₉
- (b) BaFe₁₀Cr₂O₁₉
- (c) BaF₈Cr₄O₁₉

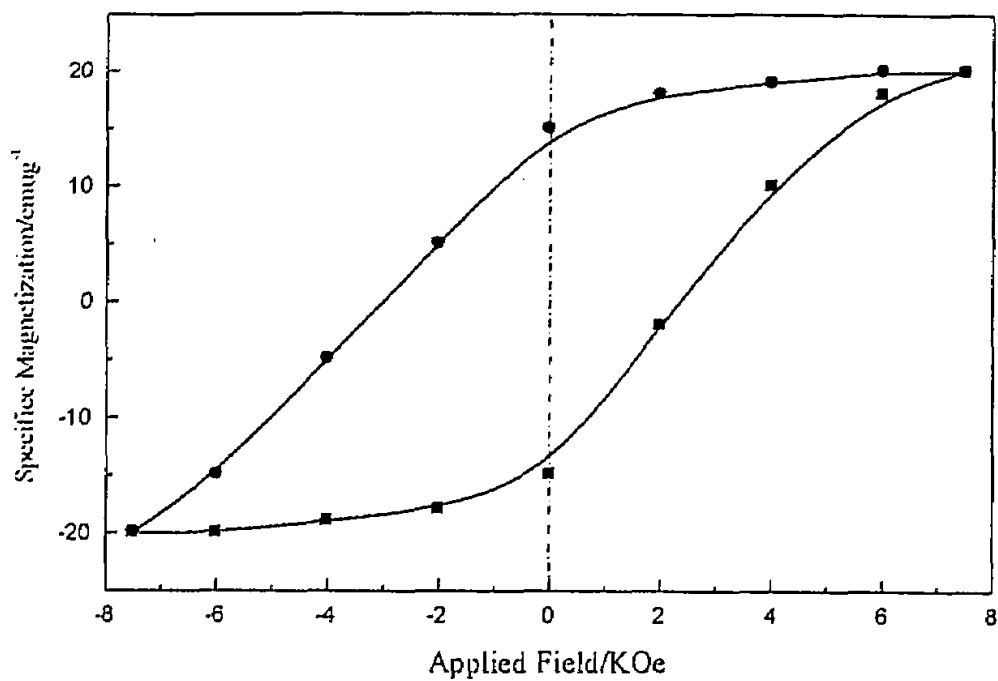


Figure 5. Hysteresis loops for sintered BaFe₁₀Cr₂O₁₉, prepared by SHS reaction

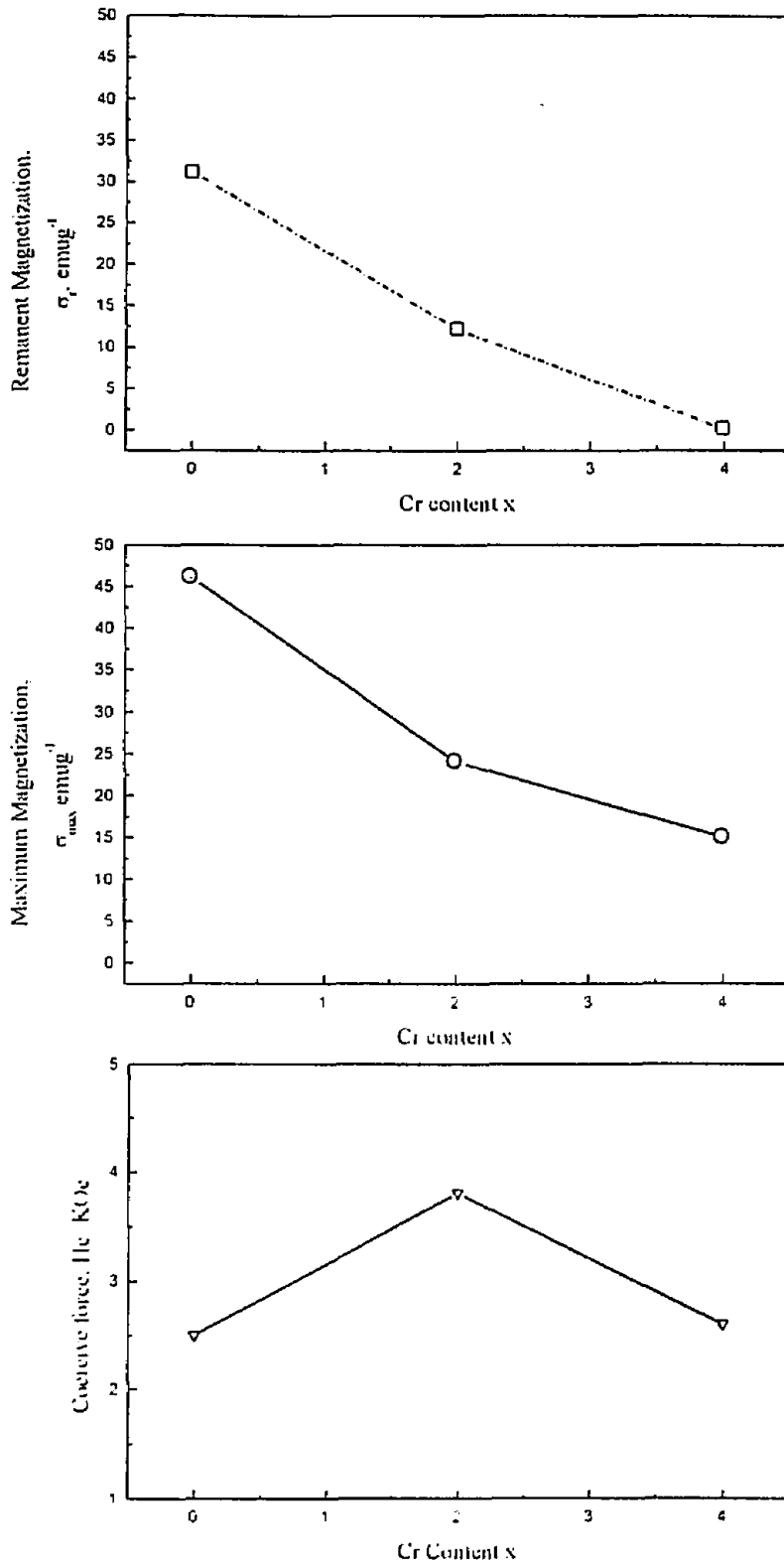


Figure 6: Magnetic properties of $BaFe_{12-x}Cr_xO_{19}$ prepared by SHS measured at 7.5 Koe at room temperature

FIGURE CAPTIONS

Fig. 1 Photographs of wave produced on initiating a mixture of BaO_2 , Fe_2O_3 , and Cr_2O_3 (1:1.6:4.8 molar ratio) at (a) time, = 0; (b) time = 50 second, (c) time = 90 second and (d) the end of SHS reaction. The mixture was initiated by a hot filament at the right side of powder.

Fig. 2. X-ray diffraction pattern obtained from SHS reaction of BaO_2 , Fe_2O_3 , Fe and Cr_2O (1:1.6:4.8:0.8 molar ratio)

a- before sintering

b- after sintering 2h at 1200°C

c- XRD pattern of commercial sample $\text{BaFe}_{12}\text{O}_{19}$

Fig. 3. FT – IR spectra of synthesized ferrites by SHS reactions,

(a) $\text{BaFe}_{12}\text{O}_{19}$

(b) $\text{BaFe}_{10}\text{Cr}_2\text{O}_{19}$

(c) $\text{BaFe}_8\text{Cr}_4\text{O}_{19}$

Fig. 4. SEM micrographs of synthesized ferrites by SHS reactions followed by sintering at 1200°C for 1 hr.

(a) $\text{BaFe}_{12}\text{O}_{19}$

(b) $\text{BaFe}_{10}\text{Cr}_2\text{O}_{19}$

(c) $\text{BaFe}_8\text{Cr}_4\text{O}_{19}$

Figure 5. Hysteresis loops for sintered $\text{BaFe}_{10}\text{Cr}_2\text{O}_{19}$, prepared by SHS reaction

Figure 6: Magnetic properties of $\text{BaFe}_{12-x}\text{Cr}_x\text{O}_{19}$ prepared by SHS measured at 7.5 Koe at room temperature